Scilight

Journal of Applied Mathematics, Mechanics and Engineering
https://www.sciltp.com/journals/jamme

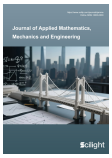

Article

Heat Transfer Analysis of MHD Quiescent Couple-Stress Non-Newtonian Flow in a Porous Medium over a Stretching/Shrinking Sheet under PST and PHF Conditions: A Numerical Approach

Sina Sadighi [1], Marin Marin [1,*] and Sorin Vlase [2]

[1] Department of Mathematics and Computer Science, Transilvania University of Brasov, 500036 Brasov, Romania
[2] Department of Mechanical Engineering, Transilvania University of Brasov, 500036 Brasov, Romania
* Correspondence: m.marin@unitbv.ro

How To Cite: Sadighi, S.; Marin, M.; Vlase, S. Heat Transfer Analysis of MHD Quiescent Couple-Stress Non-Newtonian Flow in a Porous Medium over a Stretching/Shrinking Sheet under PST and PHF Conditions: A Numerical Approach. *Journal of Applied Mathematics, Mechanics and Engineering* **2026**, *1*(1), 2.

Received: 19 November 2025
Revised: 9 December 2025
Accepted: 7 January 2026
Published: 21 January 2026

Abstract: This numerical investigation examines the behavior of a quiescent couple-stress fluid and the associated heat transfer phenomena on a stretching/shrinking cylinder subjected to specified surface temperature and heat flux boundary conditions. It is founded on the similarity solution that highly non-linear partial differential equations (PDEs) can be simplified to highly non-linear ordinary differential equations (ODEs). The problem involves several parameters, including couple stress, suction/injection, magnetic field inclination, stretching/shrinking, heat source/sink, radiation parameters, as well as the Hartmann, Darcy, Prandtl, and Eckert numbers. The reduced ODEs were numerically simulated utilizing Maple. The temperature profiles and local Nusselt numbers for various boundary conditions are compared using plots and tables. The results indicated that the impact of prescribed heat flux on reducing the local Nusselt number is significantly greater than that of prescribed surface temperature for a given Eckert number. Also, under PST, the local Nusselt number rises more with s than under PHF.

Keywords: numerical solutions; quiescent couple-stress; PST; PHF; porous surface; Nusselt number

1. Introduction

Many engineering and biomechanical processes, such as lubricants with additives, polymeric suspensions, blood flow at the microscale, and advanced manufacturing fluids used in coating and extrusion, involve flows of quiescent couple-stress fluids, where microstructural effects and particle rotation are significant. In modeling magnetohydrodynamic (MHD) systems—such as electromagnetic casting, crystal growth, magnetic drug targeting, and MHD pumps with tunable field angles—the inclusion of an inclined magnetic field is crucial, as its orientation affects flow control and thermal transport. Viscous dissipation is an essential characteristic because it involves the transformation of kinetic energy into thermal energy through internal friction. This phenomenon holds particular significance in applications such as lubrication systems, polymer processing, geothermal reservoirs, high-performance heat exchangers, and microfluidic devices. The boundary condition known as Prescribed Surface Temperature (PST) is applied when the surface temperature is kept at or controlled to a known value. In systems where maintaining a fixed surface temperature is essential despite variations in the surrounding fluid, this condition occurs. The boundary condition known as Prescribed Heat Flux (PHF) is especially significant in situations where external energy sources actively regulate the heat input. PHF is crucial in applications such as

laser-assisted manufacturing, induction heating, thermal insulation design, and electronic cooling, all of which require regulation of the heat supplied to the surface.

Turkyilmazoglu [1] demonstrated the existence of multiple physically relevant solution branches while examining the magnetohydrodynamic slip flow of a viscoelastic fluid over a stretching sheet. The research emphasized the impact of magnetic forces, slip conditions, and viscoelastic properties on heat and mass transfer, offering significant understanding into the nonlinear boundary-layer effects observed in flows over stretching sheets. Turkyilmazoglu [2] provided exact analytical solutions for the two-dimensional laminar flow over a sheet that continuously stretches or shrinks in a quiescent, electrically conducting fluid exhibiting couple stresses. The effects of couple-stress and magnetic fields change the boundary-layer configuration, offering precise reference points for validating numerical and approximate methods in non-Newtonian MHD flows. Ali et al. [3] examined the behavior of a couple-stress fluid undergoing magnetohydrodynamic flow and heat transfer along an oscillating stretching surface situated within a porous medium, considering the influence of an internal heat source or sink. Their findings indicated that the parameters related to couple stress, the strength of the magnetic field, and porosity notably affect both the velocity and temperature distributions, emphasizing key control factors for heat transfer within an intricate non-Newtonian porous medium. Mahabaleshwar et al. [4] examined the flow of an MHD couple-stress fluid induced by a linearly stretching perforated sheet, focusing on its heat transfer properties. The results indicated that the effects of perforation, magnetic fields, and couple-stress parameters considerably modify the momentum and heat transfer boundary layers, providing valuable insights for sophisticated manufacturing and cooling techniques. Hayat et al. [5] studied the airflow over a stretched cylinder in a thermally stratified environment, considering the effects of a variable heat source/sink and thermal radiation. Their findings showed that the distributions of thermal boundary layers are significantly affected by non-uniform spatial heat production and radiation heat transfer, highlighting the importance of these factors in scenarios involving heated cylindrical surfaces. Das et al. [6] studied the flow of a magneto-radiated, couple-stress fluid described by Darcy–Forchheimer equations over an exponentially stretching inclined surface, including effects like Ohmic dissipation and resistance from the porous medium. Their research indicated that the velocity and temperature profiles are substantially affected by the inclination of the magnetic field, nonlinear drag forces, radiation, and Joule heating, providing a more comprehensive understanding of the intricate heat transfer processes in porous MHD couple-stress flows. Gajjela and Garvandha [7] investigated the flow of a magnetized couple-stress fluid over a stretching cylinder, considering convective boundary conditions, cross-diffusion effects, and chemical reactions. The study revealed that the thermal and concentration boundary layers are notably affected by magnetic fields, couple-stress phenomena, and reactive mass transfer, offering important insights for processes involving cylindrical stretching surfaces and reactive transport. Gajjela and Nandkeolyar [8] examined the MHD flow of a dusty fluid with couple-stress characteristics along a stretching surface, accounting for viscous dissipation and suction. The findings showed that the interaction between dust and fluid, magnetic influences, and internal resistance play a crucial role in modifying the velocity and temperature distributions, providing further insight into the dissipative heating processes in non-Newtonian flows containing particles. Reddy et al. [9] investigated the unsteady flow of an MHD couple-stress fluid emanating from a shrinking porous surface, using the variation iteration method to obtain approximate analytical solutions. The study demonstrated that momentum and thermal profiles are significantly influenced by unsteadiness, magnetic fields, permeability, and couple-stress effects, offering useful benchmarks for time-dependent non-Newtonian porous flows. This study [10] examined the flow of an MHD nanofluid over a porous sheet that is either stretching or shrinking, incorporating mass transpiration and the Brinkman number. The authors concluded that increases in the Brinkman ratio and magnetic parameter lead to higher effective viscosity and reduced velocity. In contrast, heat and mass transfer rates are strongly affected by suction/injection. Sneha et al. [11] examined the influence of couple stress and mass transpiration on the flow dynamics and heat transfer characteristics of a ternary hybrid nanoliquid over a stretching/shrinking sheet. The momentum and thermal boundary layers are significantly influenced by couple-stress parameters and suction/injection, which in turn enhances control over heat transport in hybrid nanofluid systems. The influence of thermal radiation on the flow and heat transfer properties of a Boussinesq couple-stress nanofluid over a porous nonlinear stretching sheet was analyzed by Mahabaleshwar et al. [12]. They concluded that thermal radiation greatly amplifies the temperature field and alters the thermal boundary-layer thickness, highlighting its significant role in porous nanofluid transport. Rehman et al. [13] studied the effects of Marangoni convection, solar radiation, and viscous dissipation on a hybrid nanofluid flow with bioconvection and couple-stress properties over a shrinking surface. They concluded that the temperature field is substantially increased by solar radiation and viscous dissipation, while Marangoni convection significantly influences both fluid motion and heat transfer. Tarakaramu et al. [14] examined the flow of a 3-D Non-Newtonian couple-stress fluid over a permeable, stretching surface, accounting for nonlinear thermal radiation and internal heat sources. They found that the heat transfer behavior of couple-stress fluids is greatly affected by the nonlinear radiation and heat generation, which significantly increases the temperature field and alters the three-dimensional boundary-

layer structure. Khan et al. [15] investigated the entropy generation in a magneto–couple-stress bionanofluid flow that contains gyrotactic microorganisms, occurring near a stagnation point on a sheet that is either stretching or shrinking. They found that the behavior of the thermal and momentum boundary layers is significantly influenced by magnetic effects, couple-stress parameters, and microorganism activity, which also affect entropy production. Investigating the impact of thermal radiation on MHD couple-stress hybrid nanofluid flow over a porous sheet, Mahesh et al. [16] also incorporated the effects of viscous dissipation. They demonstrated that radiation and viscous dissipation have a strong influence on the behavior of hybrid nanofluid in a porous medium, significantly raising the temperature field and altering heat-transfer rates. Mahesh et al. [17] investigated the influence of an inclined magnetic field on the flow of couple-stress fluid over a stretching surface, incorporating Stefan blowing, thermal radiation, and chemical reactions. They concluded that both velocity and temperature fields are significantly influenced by magnetic field inclination, injection, and radiation, whereas chemical reactions have a notable effect on concentration distributions. Byeon et al. [18] investigated the lubrication of a couple-stress fluid in a magnetohydrodynamic squeeze film between rough flat and curved circular sheets, accounting for viscosity variations. They found that the load-carrying capacity is significantly increased and the pressure distribution within the squeeze-film region is affected by couple-stress effects, magnetic fields, and surface roughness. Prandtl–Eyring couple-stress fluid flow through a porous region over a stretched porous sheet was analyzed by Moatimid et al. [19], considering both homogeneous and heterogeneous chemical reactions, while taking into account these factors. They demonstrated that the concentration and velocity fields are significantly influenced by couple-stress effects and reactive species interactions, showing a strong coupling between chemical reactions and porous-medium transport. Rehman et al. [20] examined the flow and heat transfer behavior of Williamson nanofluid with couple-stress effects toward a shrinking surface, considering slip conditions and viscous dissipation. Their conclusion was that the temperature field is significantly increased and the velocity profile is changed due to the strong influence of viscous dissipation and slip, demonstrating their impact on the heat-transfer performance in Williamson–couple-stress nanofluids. Mushahary et al. [21] studied the thermal behavior of a hybrid nanofluid flow that includes magnetohydrodynamic and couple-stress effects, passing through a porous medium while also considering Hall and ion-slip phenomena. They concluded that the flow rotation and temperature distribution are markedly enhanced and modified by Hall current and ion-slip, respectively. Additionally, heat-transfer characteristics are significantly influenced by couple-stress and porous-medium resistance. Turkyilmazoglu [22] investigated the flow of a viscoelastic fluid in a hydromagnetic permeable medium, emphasizing nonlinear dynamics and the potential for multiple boundary-layer solutions. He concluded that the stability and structure of the solutions are strongly influenced by magnetic and permeability parameters, and that the system admits multiple physically acceptable solution branches. This field is actively being researched worldwide every day [23–33].

This study aims to gain a clearer understanding of the distinctions between two thermal boundary conditions applied to a quiescent couple-stress fluid. Additionally, the results, compared with various references to verify the outcomes and other tabular data, may assist future research. Many significant studies have been conducted on non-Newtonian fluids, but there remains much to explore regarding a quiescent couple-stress fluid. The novelty of this study lies in the comparison of the characteristics of quiescent couple-stress fluid flow and heat transfer on a stretching/shrinking porous sheet embedded within a porous medium, under two distinct thermal boundary conditions. Several parameters, including magnetic field, porous medium, viscous dissipation, and heat source/sink, were considered. The motivation for this study is primarily the extensive applications of quiescent couple-stress fluids, which have served as the impetus for conducting this research.

2. Mathematical Formulation

This study investigates the flow of a quiescent couple-stress fluid over a porous stretching or shrinking cylinder. The physical phenomena are depicted in Figure 1.

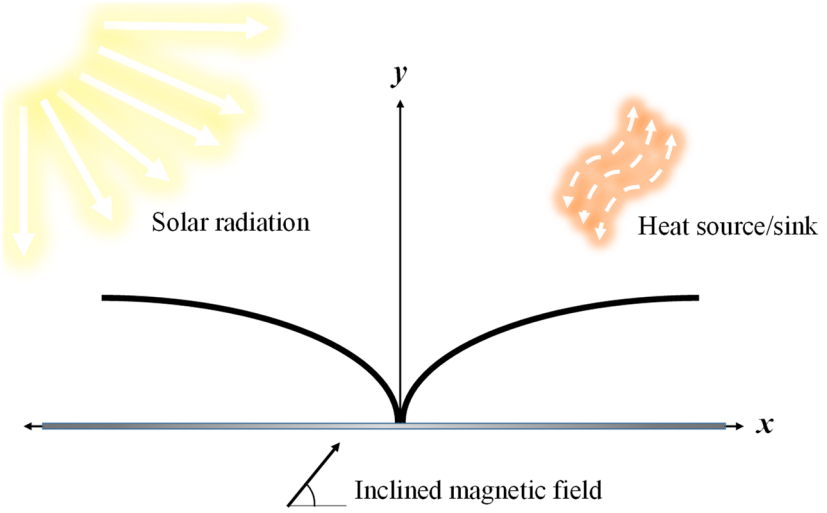

Figure 1. Schematic depiction of the problem.

The governing equations of continuity, momentum, and energy within the boundary layer, as described by the Rosseland approximation, are articulated as follows [16]:

$$\frac{\partial u}{\partial x}+\frac{\partial v}{\partial y}=0, \tag{1}$$

$$u\frac{\partial u}{\partial x}+v\frac{\partial u}{\partial y}=\frac{\mu_f}{\rho_f}\frac{\partial^2 u}{\partial y^2}-\frac{\eta_0}{\rho_f}\frac{\partial^4 u}{\partial y^4}-\frac{\sigma_f}{\rho_f}B_0^2\sin^2(\alpha)u-\frac{\mu_f}{\rho_f k}u, \tag{2}$$

$$\begin{aligned}u\frac{\partial T}{\partial x}+v\frac{\partial T}{\partial y}&=\frac{\mu_f}{(\rho c_p)_f}\left(\frac{\partial u}{\partial y}\right)^2+\frac{k_f}{(\rho c_p)_f}\left(\frac{\partial^2 T}{\partial y^2}\right)+\frac{\sigma_f}{(\rho c_p)_f}B_0^2\sin^2(\alpha)u^2+\frac{\mu_f}{(\rho c_p)_f k}u^2\\&+\frac{1}{(\rho c_p)_f}\left(\frac{16\sigma^* T_\infty^3}{3K^*}\frac{\partial^2 T}{\partial y^2}\right)+\frac{Q_0(T-T_\infty)}{(\rho c_p)_f}+\frac{\eta_0}{(\rho c_p)_f}\left(\frac{\partial^2 u}{\partial y^2}\right)^2\end{aligned} \tag{3}$$

Regarding the boundary conditions, the following apply:

$$y=0\begin{cases}u=u_w(x)=adx, v=-V_w,\\ T=T_w(x)=T_\infty+Ax^2\ (PST\ case),\\ q_w(x)=-k\dfrac{\partial T}{\partial y}=Bx^2\ (PHF\ case),\end{cases} \tag{4}$$

$$u\to 0,\ \ T\to T_\infty \qquad \text{as } y\to\infty, \tag{5}$$

The fluid temperature is T, and its velocities in the $-x$ and $-y$ directions are u and v, respectively. Additionally, V_w denotes the porosity of the surface that stretches or shrinks, used for transferring quiescent couple-stress fluid. To model the fluid dynamics and heat transfer phenomena occurring on a porous stretching or shrinking surface, the relevant similarity variables are given in [34].

$$\eta=y\sqrt{\frac{a}{\nu_f}}, u=axf'(\eta), v=-\sqrt{a\nu_f}f(\eta), PST:\theta(\eta)=\frac{T-T_\infty}{T_w-T_\infty}, PHF:T=T_\infty+\frac{q_w}{k_f}\sqrt{\frac{\nu_f x}{u_w(x)}}\theta(\eta) \tag{6}$$

When similarity solutions are used to solve PDEs, the resulting equations are highly nonlinear coupled ODEs, as follows:

$$-Cf''''+ff''+f'^2-(Ha\sin^2(\alpha)+Da)f'=0 \tag{7}$$

$$(1+Rd)\theta''+Pr\left\{f\theta'-2f'\theta+Ec\left[Cf'''^2+f''^2+(Ha\sin^2(\alpha)+Da)f'^2\right]+Q\theta\right\}=0 \tag{8}$$

The simplified boundary conditions are:

$$f(0)=s,\ \ f'(0)=d,\ \ PST:\theta(0)=1,\ \ PHF:\theta'(0)=-1 \tag{9}$$

$$f'(\infty)\to 0,\ \ f''(\infty)\to 0, f'''(\infty)\to 0, \theta(\infty)\to 0, \tag{10}$$

The local skin friction coefficient and local Nusselt number are expressed in PDE form as follows [15]:

$$C_f = \frac{\mu_f}{\rho_f u_w^2}\left(\frac{\partial u}{\partial y} - \frac{\eta_0}{\rho_f}\frac{\partial^3 u}{\partial y^3}\right)_{y=0}, Nu_x = \frac{q_w x}{k_f(T_w - T_\infty)}\left(\frac{\partial T}{\partial y}\right)_{y=0} \quad (11)$$

The reduced local skin friction coefficient and local Nusselt number, expressed as ODE forms, are obtained after employing similarity variables:

$$Re_x^{1/2} C_f = f''(0) - Cf''''(0), \;\; PST: Re_x^{-1/2} Nu_x = -(1 + Rd)\theta'(0), \;\; PHF: Re_x^{-1/2} Nu_x = \frac{1}{\theta(0)} \quad (12)$$

3. Results and Discussion

The issue pertains to the flow and heat transfer of a quiescent couple-stress fluid over a porous stretching/shrinking surface under two specified thermal boundary conditions. In Maple, the Runge-Kutta-Fehlberg approach combined with a shooting method is used to numerically solve the highly nonlinear ordinary differential equations.

Figure 2 illustrates that suction with $s = +2$ cools and reduces the thickness of the thermal layer, whereas injection warms and thickens it; an intermediate condition occurs at $s = 0$. PST results in higher temperatures than PHF for each s: since PST maintains a fixed wall temperature, the surface remains hot, allowing thermal energy to penetrate more deeply, which leads to a thicker TP. Under PHF, the surface temperature can decrease, and lower temperatures throughout the layer can be achieved because the wall heat flux is prescribed, which constrains the near-wall gradient. Although the couple-stress parameter introduces microstructural effects, it does not alter the ordering imposed by s and the boundary condition.

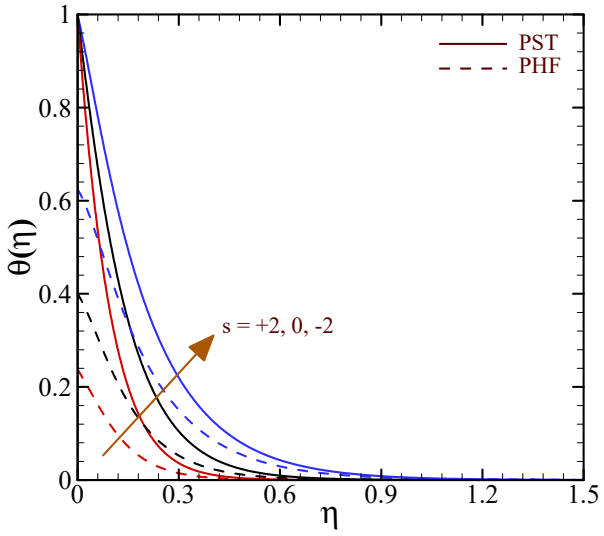

Figure 2. Effects of suction/injection parameter on the temperature profile when $C = 0.01, d = 1, Ha = 2, \alpha = \pi/2, Da = 0.05, Pr = 6.2, Rd = 1, Q = -20,$ and $Ec = 0.1$.

The temperature distribution under suction for both PST and PHF boundary conditions is illustrated in Figure 3, showing the effect of the radiation parameter. As the radiation parameter increases from 0 to 4, the temperature profiles experience a significant rise, illustrating the well-known effect of thermal radiation that adds extra energy to the fluid and consequently thickens the thermal boundary layer. Since prescribing the wall temperature results in higher temperatures throughout the boundary layer than prescribing the wall heat flux, the PST curves lie above the PHF curves for every value of Rd. According to boundary condition theory, this behavior occurs because PST sets a high, dimensionless wall temperature, promoting deeper diffusion of thermal energy into the flow. In contrast, PHF constrains the heat-flux gradient at the wall, allowing the wall temperature to decrease and resulting in a cooler thermal field. The plot clearly demonstrates that heat transfer is significantly influenced by both radiation and the type of thermal boundary condition, with radiation increasing temperature and PST ensuring the highest thermal levels throughout the boundary layer.

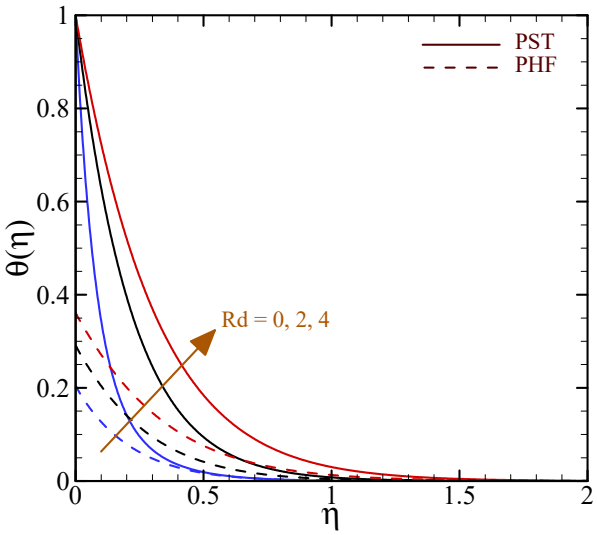

Figure 3. Effects of radiation parameter on the temperature profile when $s = 2, C = 0.05, d = -1, Ha = 3, \alpha = \pi/4, Da = 0.07, Pr = 6.2, Q = -5,$ and $Ec = 0.2$.

Because a positive heat source injects additional thermal energy into the boundary layer, increasing Q from -6 to $+6$ raises the temperature profile significantly, as expected in Figure 4. A heat sink cools the flow by extracting energy, unlike what is described otherwise. Regarding each value of Q, the PST curves are positioned above the PHF curves, signifying that establishing the surface temperature at a designated level results in an elevated near-wall temperature and an augmented thermal boundary layer. Conversely, when a heat flux is specified, the wall temperature is permitted to adapt to a lower value, thereby generating a comparatively cooler temperature distribution. The curves are ordered consistently with respect to Q: heat sinks lead to a reduction in TP, thermal neutrality $(Q = 0)$ is positioned in the middle, and heat sources produce the highest temperature profiles. The figure clearly illustrates the significant thermal effect of the heat source/sink parameter and differentiates the regulation of near-wall heat transfer under PST and PHF conditions for a magnetized, porous, couple-stress flow over a shrinking surface.

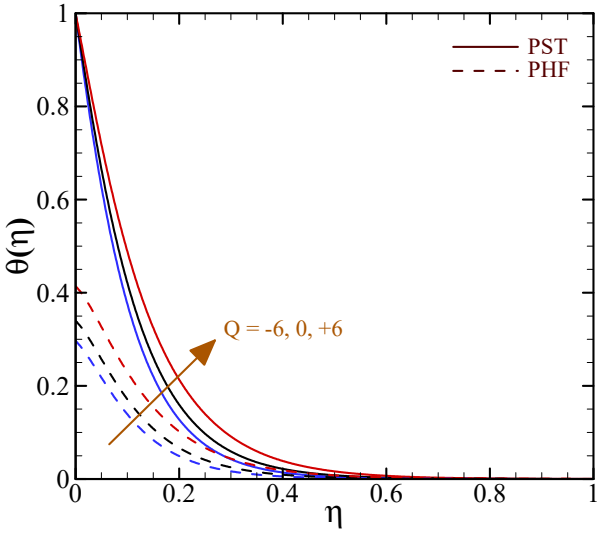

Figure 4. Effects of heat source/sink parameter on the temperature profile when $s = 5, C = 0.004, d = -2, Ha = 5, \alpha = \pi/6, Da = 0.01, Pr = 6.2, Rd = 2,$ and $Ec = 0.03$.

As illustrated in Figure 5, an increase in Ec from 0 to 1 appears to elevate TP, since a higher Eckert number enhances viscous dissipation—the process converting kinetic energy into internal thermal energy within the boundary layer. Because the thermal boundary layer thickens and the fluid temperature increases due to this additional heat generation, the red curves are positioned above the black and blue curves. The PST curves stay higher than the corresponding PHF curves across all Eckert-number values. Because PST sets the wall temperature at a specified value, it permits thermal energy to penetrate more deeply into the flow, making this behavior expected. Conversely, PHF only sets the surface heat flux, which causes the wall temperature to decrease and leads

to a cooler thermal field. Figure 5 accurately depicts two consistent physical trends: first, that increasing viscous dissipation enhances heating within the boundary layer, and second, that under identical flow and thermal parameters, PST exhibits a hotter and thicker thermal layer compared to PHF.

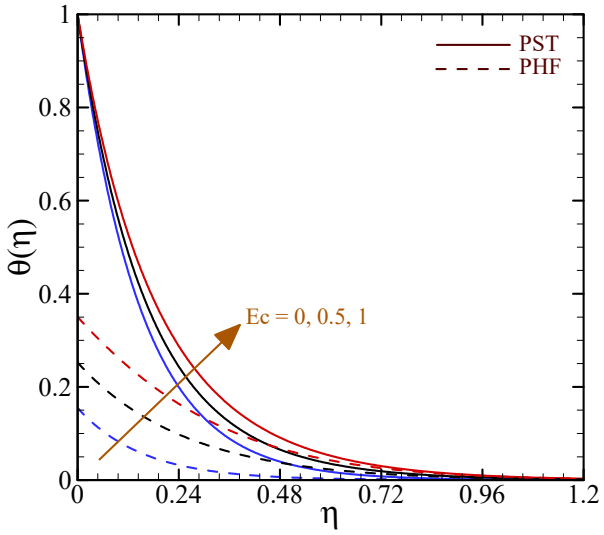

Figure 5. Effects of Eckert number on the temperature profile when $s = 1, C = 0.1, d = 1, Ha = 1, \alpha = \pi/3, Da = 0.03, Pr = 6.2, Rd = 3,$ and $Q = -20$.

A comparison was made between the current results and those of earlier studies [2,35,36]. Table 1 shows some values of Pr and the heat transfer rate in this regard. The table shows an excellent agreement.

Table 1. Local Nusselt number comparison between [2,35,36].

Pr	Nataraja et al. [35]	Mushtaq et al. [36]	Turkyilmazoglu [2]	Present
1	1.3333	1.3349	1.333333	1.33333333
5	3.3165	3.2927	3.316482	3.31648250
10	4.4769	4.7742	4.796873	4.79687328
15	5.9320	5.9097	5.932011	5.93201065
100	15.7120	15.6884	15.71197	15.7119671
400	31.6990	31.6289	31.67049	31.6704624

4. Conclusions

The problem involving quiescent couple-stress fluid flow and heat transfer was simulated using numerical methods. The comparison involved two thermal boundary conditions, PST and PHF. Numerical simulation of the problem was carried out using the appropriate similarity variables, which were selected based on the boundary conditions. The profiles are depicted by the effects of parameters. According to the research, the subsequent inferences can be made:

- The Eckert number, injection, radiation, and heat source parameters directly influence the temperature profiles.
- Under PST, the increase in the local Nusselt number with changing s is greater than that under PHF.
- Increasing Rd increases the local Nusselt number in PST while decreasing it in PHF.
- An increase in Q results in a greater decrease in the local Nusselt number within PST compared to PHF.
- By increasing $\boldsymbol{Ec}$, the local Nusselt number for PHF decreased by approximately 2 times compared to PST.

Author Contributions

All authors contributed equally to the conception, editing and proofreading of the manuscript. All authors have read and agreed to the published version of the manuscript.

Funding

This research received no external funding.

Institutional Review Board Statement

Our study did not involve humans or animals.

Informed Consent Statement

Not applicable.

Data Availability Statement

Authors can provide the raw data of their study along with the manuscript for editorial review and are prepared to make the data available to the public, provided that copyright is respected, upon request to the corresponding author.

Conflicts of Interest

The authors declare no conflict of interest.

Use of AI and AI-Assisted Technologies

No AI tools were utilized for this paper.

References

1. Turkyilmazoglu, M. Multiple solutions of heat and mass transfer of MHD slip flow for the viscoelastic fluid over a stretching sheet. *Int. J. Therm. Sci.* **2011**, *50*, 2264–2276.
2. Turkyilmazoglu, M. Exact solutions for two-dimensional laminar flow over a continuously stretching or shrinking sheet in an electrically conducting quiescent couple stress fluid. *Int. J. Heat Mass Transf.* **2014**, *72*, 1–8.
3. Ali, N.; Khan, S.U.; Sajid, M.; et al. MHD flow and heat transfer of couple stress fluid over an oscillatory stretching sheet with heat source/sink in porous medium. *Alex. Eng. J.* **2016**, *55*, 915–924.
4. Mahabaleshwar, U.S.; Sarris, I.E.; Hill, A.A.; et al. An MHD couple stress fluid due to a perforated sheet undergoing linear stretching with heat transfer. *Int. J. Heat Mass Transf.* **2017**, *105*, 157–167.
5. Hayat, T.; Asad, S.; Alsaedi, A. Non-uniform heat source/sink and thermal radiation effects on the stretched flow of cylinder in a thermally stratified medium. *J. Appl. Fluid Mech.* **2017**, *10*, 915–924.
6. Das, S.; Ali, A.; Jana, R.N. Darcy–Forchheimer flow of a magneto-radiated couple stress fluid over an inclined exponentially stretching surface with Ohmic dissipation. *World J. Eng.* **2021**, *18*, 345–360.
7. Gajjela, N.; Garvandha, M. The influence of magnetized couple stress heat, and mass transfer flow in a stretching cylinder with convective boundary condition, cross-diffusion, and chemical reaction. *Therm. Sci. Eng. Prog.* **2020**, *18*, 100517.
8. Gajjela, N.; Nandkeolyar, R. Investigating the magnetohydrodynamic flow of a couple stress dusty fluid along a stretching sheet in the presence of viscous dissipation and suction. *Heat Transf.* **2021**, *50*, 2709–2724.
9. Reddy, G.J.; Hiremath, A.; Kumar, M.; et al. Unsteady magnetohydrodynamic couple stress fluid flow from a shrinking porous sheet: Variational iteration method study. *Heat Transf.* **2022**, *51*, 2219–2236.
10. Anusha, T.; Mahabaleshwar, U.S.; Sheikhnejad, Y. An MHD of nanofluid flow over a porous stretching/shrinking plate with mass transpiration and Brinkman ratio. *Transp. Porous Media* **2022**, *142*, 333–352.
11. Sneha, K.N.; Vanitha, G.P.; Mahabaleshwar, U.S.; et al. Effect of couple stress and mass transpiration on ternary hybrid nanoliquid over a stretching/shrinking sheet with heat transfer. *Micromachines* **2022**, *13*, 1694.
12. Mahabaleshwar, U.S.; Vishalakshi, A.B.; Bognar, G.V.; et al. Effect of thermal radiation on the flow of a Boussinesq couple stress nanofluid over a porous nonlinear stretching sheet. *Int. J. Appl. Comput. Math.* **2022**, *8*, 169.
13. Rehman, A.; Khan, W.; Abdelrahman, A.; et al. Influence of Marangoni convection, solar radiation, and viscous dissipation on the bioconvection couple stress flow of the hybrid nanofluid over a shrinking surface. *Front. Mater.* **2022**, *9*, 964543.
14. Tarakaramu, N.; Satya Narayana, P.V.; Sivajothi, R.; et al. Three-dimensional non-Newtonian couple stress fluid flow over a permeable stretching surface with nonlinear thermal radiation and heat source effects. *Heat Transf.* **2022**, *51*, 5348–5367.
15. Khan, M.S.; Shah, Z.; Roman, M.; et al. Entropy generation in magneto couple stress bionanofluid flow containing gyrotactic microorganisms towards a stagnation point on a stretching/shrinking sheet. *Sci. Rep.* **2023**, *13*, 21434.
16. Mahesh, R.; Mahabaleshwar, U.S.; Kumar, P.V.; et al. Impact of radiation on the MHD couple stress hybrid nanofluid flow over a porous sheet with viscous dissipation. *Results Eng.* **2023**, *17*, 100905.

17. Mahesh, R.; Vishalakshi, A.B.; Mahabaleshwar, U.S.; et al. Impact of an inclined magnetic field on couple stress fluid flow over a stretching surface with effect of Stefan blowing, radiation and chemical reaction. *J. Magn. Magn. Mater.* **2023**, *580*, 170953.
18. Byeon, H.; Latha, Y.L.; Hanumagowda, B.N.; et al. Magnetohydrodynamics and viscosity variation in couple stress squeeze film lubrication between rough flat and curved circular plates. *Sci. Rep.* **2023**, *13*, 22960.
19. Moatimid, G.M.; Mohamed, M.A.; Elagamy, K. Prandtl-Eyring couple stressed flow within a porous region counting homogeneous and heterogeneous reactions across a stretched porous sheet. *Partial. Differ. Equ. Appl. Math.* **2024**, *10*, 100706.
20. Rehman, A.; Khun, M.C.; Inc, M.; et al. Analytical simulation for couple stress Williamson nanofluid flow and heat transfer towards a shrinking surface with slip and viscous dissipation effects. *J. Appl. Math. Mech.* **2025**, *105*, e202400890.
21. Mushahary, P.; Ontela, S. Thermal analysis of magnetohydrodynamic couple-stress hybrid nanofluid flow in porous medium with Hall and ion-slip effects. *Multiscale Multidiscip. Model. Exp. Des.* **2025**, *8*, 205.
22. Turkyilmazoglu, M. Multiple solutions of hydromagnetic permeable flow and heat for viscoelastic fluid. *J. Thermophys. Heat Transf.* **2011**, *25*, 595–605.
23. Zeeshan, A.; Khan, M.I.; Ellahi, R.; et al. Computational intelligence approach for optimising MHD Casson ternary hybrid nanofluid over the shrinking sheet with the effects of radiation. *Appl. Sci.* **2023**, *13*, 9510.
24. Akram, J.; Zeeshan, A.; Alhodaly, M.S.; et al. Evaluation of magnetohydrodynamics of natural convective heat flow over circular cylinder saturated by nanofluid with thermal radiation and heat generation effects. *Mathematics* **2022**, *10*, 1858.
25. Sadighi, S.; Afshar, H.; Jalili, P.; et al. Thermal analysis of Al_2O_3/H_2O nanofluid flow on a porous stretching/shrinking cylinder: Implications for biomedical applications under convective boundary conditions. *Multiscale Multidiscip. Model. Exp. Des.* **2025**, *8*, 400.
26. Sadighi, S.; Afshar, H.; Jalili, P.; et al. Heat transfer analysis of fluid flow over a nonlinear porous radially moving sheet: Benchmark solutions. *Case Stud. Therm. Eng.* **2025**, *65*, 105707.
27. Ahmed, B.; Abbas, M.A.; Rehman, S.U.; et al. Numerical investigation of entropy generation on MHD flow of micropolar fluid over a stretching sheet in the presence of a porous medium. *Waves Random Complex Media* **2025**, *35*, 3738–3752.
28. Marin, M. Generalized solutions in elasticity of micropolar bodies with voids. *Rev. De La Acad. Canar. De Cienc. Folia Canar. Acad. Sci.* **1996**, *8*, 101–106.
29. Mahabaleshwar, U.S.; Maranna, T.; Huang, H.N.; et al. An impact of MHD and radiation on Boussinesq–Stokes suspensions fluid flow past a porous flat plate with mass suction/injection. *J. Therm. Anal. Calorim.* **2025**, *150*, 2517–2532.
30. Basha, H.; Naduvinamani, N.B.; Shridhar, M. Numerical analysis of velocity slip and magnetic Soret effect on dissipative Maxwell liquid motion about a stretching wall with heat source/sink. *Numer. Heat Transf. Part B Fundam.* **2025**, *86*, 2721–2745.
31. Sadighi, S.; Marin, M. An in-depth theoretical investigation of biomagnetic fluid flow and heat-mass transfer on a porous stretching/shrinking cylinder hosting motile gyrotactic microorganisms. *Int. J. Numer. Methods Heat Fluid Flow* 2025, 1–22. https://doi.org/10.1108/HFF-09-2025-0671.
32. Kumar, P.; Prashu Nandkeolyar, R. Modeling the hydromagnetic transient three-dimensional stagnation point flow of a couple stress Casson fluid over a bi-directional stretching sheet. *Numer. Heat Transf. Part B Fundam.* **2025**, *86*, 1177–1195.
33. Zainal, N.A.; Mokhtar, D.M.; Waini, I.; et al. Mixed convection of couple stress hybrid nanofluid past a vertical shrinking plate. *J. Therm. Anal. Calorim.* **2025**, *150*, 8073–8081.
34. Sadighi, S.; Afshar, H.; Jabbari, M.; et al. Heat and mass transfer for MHD nanofluid flow on a porous stretching sheet with prescribed boundary conditions. *Case Stud. Therm. Eng.* **2023**, *49*, 103345.
35. Nataraja, H.R.; Sarma, M.S.; Rao, B.N. Flow of a second-order fluid over a stretching surface having power-law temperature. *Acta Mech.* **1998**, *128*, 259–262.
36. Mushtaq, M.; Asghar, S.; Hossain, M.A. Mixed convection flow of second grade fluid along a vertical stretching flat surface with variable surface temperature. *Heat Mass Transf.* **2007**, *43*, 1049–1061.